

# Numerical analysis of variable polarity arc weld pool<sup>†</sup>

Hunchul Jeong, Kyunbae Park and Jungho Cho<sup>\*</sup>

*School of Mechanical Engineering, Chungbuk National University, Cheongju 28644, Korea*

(Manuscript Received January 17, 2016; Revised April 12, 2016; Accepted May 2, 2016)

## Abstract

Aluminum alloys are the materials which face difficulties in weldability. One of solutions to increase the weldability of aluminum alloys is removing the oxide-layer on the surface of aluminum by adopting variable polarity arc welding. The authors' previous experimental research about variable polarity arc welding of aluminum showed that reverse arc polarity has larger heat input efficiency than straight polarity. In this study, numerical analysis of molten pool in aluminum alloy by variable polarity GTAW has been introduced and developed. The arc heat source, arc pressure, electromagnetic force and Marangoni flow regarding the variable polarity GTAW have been applied as the boundary conditions and body force terms. Governing equations such as the conservation of the mass, momentum and energy are numerically solved to derive temperature and flow vector field. Additionally, volume of fluid method is adopted to track free surface of molten pool and it was implemented through using commercial package Flow-3D. Through the present analysis, mathematical model for variable polarity arc is newly suggested and following result successfully showed effect of different heat input efficiency for each straight and reverse polarity. The heat input efficiencies are arbitrarily decided here for feasibility but a methodology to numerically determine the exact value is suggested. The final goal of these research series is to determine the heat input efficiency of reverse polarity arc aluminum welding indirectly through simulation and experiment comparison.

*Keywords:* Aluminum; Arc; Flow-3D; GTAW; Heat input efficiency; Variable polarity; Volume of fluid

## 1. Introduction

Aluminum alloys are well known as low weldability materials due to the high heat conductivity, thermal expansion coefficient, high sensitivity of hot crack, different solubility of the hydrogen content between solid and liquid phase [1] and the existence of the oxide-layer on surface. Except for the oxide film layer on the surface, the rest are inherent characteristic sources of low weldability. Therefore the only way to increase the weldability on the material's aspect is removing oxide layer before welding. It can be achieved through mechanically by using wire bush or electronically with VP (Variable polarity) arc power source. Although the mechanism is still controversial, the effect of oxide removal by reverse polarity, i.e. DCEP (Direct current electrode positive), is clear therefore GMAW (Gas metal arc welding) using DCEP and GTAW (Gas tungsten arc welding) with VP are famous solutions for arc welding aluminum alloys [2, 3]. VP refers a kind of AC arc current with periodic DCEP-DCEN switching.

According to conventional arc theory of anode heating, it has been known that straight polarity, i.e. DCEN (Direct current electrode negative), has higher heat input efficiency than

reverse polarity [4]. However, completely opposite experimental results have been reported in these days [5-7] and one of them suggested alternative theory which is combination of quantum tunneling effect and random walk of cathode spot then successfully explained the contradiction between conventional arc theory and experimental phenomena [8-10].

Arc heat input efficiency of straight polarity is generally well known through long historical experiments. However, efficiency of reverse polarity is still unknown because there were little studies about it comparing to straight polarity case. This research is about numerical analysis of weld pool in VP-GTAW of aluminum which is successive to the authors' previous experimental study. The main purpose of the simulation is to determine heat input efficiency of reverse polarity indirectly by comparing simulation to experiment. It costs a great deal of time to develop numerical model and modify it to experiment therefore the current research is confined to simulation development stage.

Numerical analysis model is basically assumed as incompressible, Newtonian and laminar flow. Governing equations are continuity equation, Navier-Stokes equation and energy equation. In addition to these three basic equations, conservative governing equation of fluid fraction is accompanied to track the free surface of fluid which is well known technique as VOF (Volume of fluid) method. With these four governing

<sup>\*</sup>Corresponding author. Tel.: +82 43 261 2445

E-mail address: junghocho@chungbuk.ac.kr

<sup>†</sup>Recommended by Associate Editor Young Whan Park

© KSME & Springer 2016

equations, the model is completed through adopting boundary conditions which can give the arc welding characteristics to the simulation such as arc heat input, arc pressure, surface tension induced shear force. The simulation model in this research is already verified through the authors' previous report [11-18]. New contribution for the simulation in here is that arc heat input model for variable polarity is suggested then confirmed.

## 2. Governing equations and boundary conditions

As aforementioned, it requires four governing equations to realize the virtual arc welding process. The first one to introduce is VOF method which estimates the volume fraction in each cell. The VOF technique is based on the variable  $F$ , a scalar denoting the volume fraction of fluid occupying in each cell and it follows conservative law. By definition,  $F$  value is equal to '0' in void cell, '1' in fully occupied cell and the intermediate values occurring in free surface elements. Conservation of  $F$  is expressed as [19]

$$\frac{DF}{Dt} = \frac{\partial F}{\partial t} + \nabla \cdot (\vec{V}F) = 0. \quad (1)$$

As mentioned before, it is assumed that the fluid for this analysis is based on the incompressible, Newtonian fluid and laminar flow. By these assumptions, the continuity equation of the mass conservation is expressed as

$$\nabla \cdot \vec{V} = 0. \quad (2)$$

Conservation equation of the momentum is also induced as the following Navier-Stokes equation [20]

$$\frac{DV}{Dt} = -\frac{1}{\rho} \nabla P + \mu \nabla^2 V + g_z [1 - \beta(T - T_m)] \quad (3)$$

where varied bouancy force along the weld pool's temperature was considered in the above Eq. (3). It is noticeable that the volume changes of which are assumed to be small enough to be negligible in Eq. (3) as referred from Boussinesq approximation.

It is important to apply the conservation equation of energy in order to accurately estimate the quantity of heat input and temperature distribution during the VP-GTAW. The energy equation is like following.

$$\frac{dh}{dt} + (\vec{V} \cdot \nabla)h = \frac{1}{\rho} \nabla \cdot (K \nabla T) \quad (4)$$

$$h = C_p \cdot T + f(T) \cdot L_f \quad (5)$$

$$f(T) = \begin{cases} 0, & \text{if } T \leq T_s \\ \frac{T - T_l}{T_l - T_s}, & \text{if } T_s < T < T_l \\ 1, & \text{if } T \geq T_l \end{cases} \quad (6)$$

where latent heat of fusion,  $L_f$  is divided into three types with respect to temperature including the solid state, mush zone and liquid state of weld pool.

The top surface on which the heat source is directly imposed is the region where the heat flux is extremely activated through the thermal conduction, convection and radiation energy emitted by the temperature itself. So it is assumed that the gradient of all physical properties on the other surfaces except for the top will be simply zero to make it sense if the materials by welding has enough thickness and width. In other words,

$$\frac{\partial \Phi}{\partial n} = 0 \quad (7)$$

where  $\Phi$  means any kind of physical properties and  $n$  denotes the normal direction of the plane.

Basically the heat loss by evaporation on the surface of the weldment should be considered. However, it is assumed that the evaporational heat loss on top surface is negligible because the arc welding has little influence on evaporation comparing to high power density process such as the laser beam, plasma and electron beam welding. Therefore the boundary condition of the top surface for heat transfer considers arc heat input, convectional and radiational heat loss only. Its mathematical expresion is like following.

$$K \frac{\partial T}{\partial n} = q_{VP\_GTAW} - h_A (T - T_\infty) - \sigma_s \varepsilon_r (T^4 - T_\infty^4). \quad (8)$$

In the above Eq. (8), second and third term on the right side indicate convectional and radiational heat loss respectively. The first term on the right side denotes heat flux of arc heat input which can be expressed as,

DCEP duration:

$$q_{VP\_GTAW} = \eta_{rel} \eta_{EN} \frac{VI}{C_A \pi r_A^2} \exp \left\{ -\frac{x^2 + y^2}{C_A r_A^2} \right\} \quad (9)$$

DCEN duration:

$$q_{VP\_GTAW} = \eta_{EN} \frac{VI}{C_A \pi r_A^2} \exp \left\{ -\frac{x^2 + y^2}{C_A r_A^2} \right\} \quad (10)$$

where  $\eta_{EN}$  denotes arc heat input efficiency of DCEN polarity which is generally known as value around 0.5. Efficiency of DCEP is not directly defined in here but it is expressed indirectly as multiplication of  $\eta_{rel}$  to  $\eta_{EN}$  therefore it means that only relative value compared to DCEN is interesting. Constant value of  $\eta_{EP}$  can be determined through thermal capacity experiment. However, in this research, the strategy to determine the  $\eta_{EP}$  is established by comparing simulation to experiment. The only interesting perspective of comparison is the shape and size of FZ (Fusion zone). As referred in introduction chapter, the experiment showed, the longer DCEP

duration, the larger FZ area. Therefore if we can match the proportional number between DCEP duty ratio and FZ area in simulation to experiment, we can determine the  $\eta_{EP}$  by derivation of  $\eta_{rel}$  regardless of absolute value of  $\eta_{EN}$ . In Eq. (10),  $V$ ,  $I$ ,  $C_A$  and  $R_A$  denotes voltage, current, Gaussian distribution constant and arc effective radius respectively.

During the arc welding process, the molten surface experiences two kind of pressure boundary condition. One is arc pressure by arc plasma flow [21] and the other is surface tension pressure. Mathematical expression of this pressure boundary condition on the top surface can be expressed like following.

$$-P + 2\mu \frac{\partial V_n}{\partial n} = -P_A + \frac{\gamma}{R_C} \tag{11}$$

$$P_A(x, y) = \frac{\mu_0 I^2}{4\pi^2 r_A^2} \exp\left\{-\frac{x^2 + y^2}{2r_A^2}\right\}. \tag{12}$$

Eq. (11) describes pressure boundary condition at the top surface and  $n$  denotes the normal direction and component. Second term on the left side in Eq. (11) means the normal stress on the weld pool as Newton’s viscosity law. In the same equation, second term on the right side describes the pressure by surface tension  $\gamma$  so  $R_C$  denotes local surface curvature. The first term on the right side is arc pressure and it is described by following Eq. (12).

One of the most interesting features of arc weld pool simulation is that the metal surface is locally melted and temperature gradient at the surface is quite significant. Therefore the slight difference in surface tension gradient can cause shear force induced flow and this phenomenon is referred as Marangoni flow. Following Eq. (13) is describing boundary condition of the Marangoni flow. Subscript  $\tau$  denotes the tangential component.

$$\mu \frac{\partial V_\tau}{\partial n} = -\frac{\partial \gamma}{\partial T} \frac{\partial T}{\partial \tau}. \tag{13}$$

Weld pool is in the middle of arc current path and the path is not straight but rather curvy and complex therefore electromagnetic force plays role as body force. Basically, the Lorentz force is cross product of current density  $J$  and magnetic field  $B$  like following [22]

$$F = J \times B. \tag{14}$$

When electrons are transmitted from cathode to anode, they are always emitted or absorbed in normal direction, i.e. current density is normal to anode or cathode surface. However, the weld pool surface always changes therefore it becomes extremely complex problem if the electromagnetic force should be derived along the free surface at every single moment. Therefore a previous research about electromagnetic force in arc welding made the solution simple with

assumption of flat top surface not free surface. Detailed descriptions for the assumptions are like following.

- (1) Arc current just flows in the normal direction on surface which has not wave pattern.
- (2) Electrical conductivity and magnetic permeability consider as only constant.

$$\frac{\partial K}{\partial T} = \frac{\partial \mu_m}{\partial T} = 0.$$

- (3) Current flux density is according to the Gaussian distribution as

$$J_z = \frac{I}{2\pi r_A^2} \exp\left(-\frac{r^2}{2r_A^2}\right).$$

- (4) Magnetic flux density in the radius direction and normal direction are zero in the cylindrical coordinator system.

- (5) The values of current flux density in the radius direction are averagely equal throughout whole normal positions.

With the above assumptions, three dimensional electromagnetic force components are simply derived like following Eq. (15)

$$F = \left(-\frac{I^2 \mu_m}{4\pi^2 r r_A^2} \exp\left(-\frac{r^2}{2r_A^2}\right) \times \left[1 - \exp\left(-\frac{r^2}{2r_A^2}\right)\right]\right) \left(1 - \frac{z}{c}\right)^2 \frac{x}{r} \hat{i} + \left(-\frac{I^2 \mu_m}{4\pi^2 r r_A^2} \exp\left(-\frac{r^2}{2r_A^2}\right) \times \left[1 - \exp\left(-\frac{r^2}{2r_A^2}\right)\right]\right) \left(1 - \frac{z}{c}\right)^2 \frac{y}{r} \hat{j} + \left(\frac{I^2 \mu_m}{4\pi^2 r^2 c} \left[1 - \exp\left(-\frac{r^2}{2r_A^2}\right)\right]^2\right) \left(1 - \frac{z}{c}\right) \hat{k}. \tag{15}$$

Simulation is applied to aluminum alloy (Al-8wt% Mg) instead of generally used commercial alloy because of lack of information about general thermophysical properties such as viscosity. Although almost required thermophysical information were easy to find about the chosen material, it was hard to find out exact data about surface tension gradient w.r.t. temperature. Therefore the property of Al 6061 is used instead which is widely quoted. All the thermophysical properties used in the simulation are listed up in Table 1.

Three dimensional analytic domain was set up with cubic cells which have 0.4 mm length of width, depth and height. Top surface is open to air, i.e. free surface, and faces arc heat input, convetional and radiational heat loss. The other five surfaces are set as ‘continuous’ which means gradient of any kind of thermophysical properties at the plane is zero as described in Eq. (7).

Arc current has variable polarity and it means DCEP and DCEN polarities are periodically repeated as shown in Fig. 1.

Table 1. Thermophysical properties of the Al-8wt%Mg.

Property	Value	Symbol
Density	2500 kg/m <sup>3</sup>	$\rho$
Thermal conductivity	81 J·m <sup>-1</sup> ·s <sup>-1</sup> ·°K	K
Specific heat	1108 J·k g <sup>-1</sup> ·°K	c
Solidus temp.	813°K	$T_s$
Liquidus temp.	898°K	$T_l$
Surface tension gradient	※ -3.5 × 10 <sup>-4</sup> Nm <sup>-1</sup> ·°C <sup>-1</sup>	$\frac{\partial \gamma_s}{\partial T}$
Arc radius	0.003 m	$r_A$
Magnetic permeability	1.26 × 10 <sup>-6</sup> · H/m	$\mu_m$
Ambient temperature	298 K	$T_\infty$
Latent heat fusion	394 kJ/kg	$L_f$
E missivity	0.2	$\epsilon_r$
Surface tension	0.89 N·m <sup>-1</sup>	$\gamma_s$
Convection coefficient	80 J·m <sup>-1</sup> ·s <sup>-1</sup> ·°K	$h_A$
Viscosity	0.0013 N·s·m <sup>-2</sup>	$\mu$

※ Property of Al6061

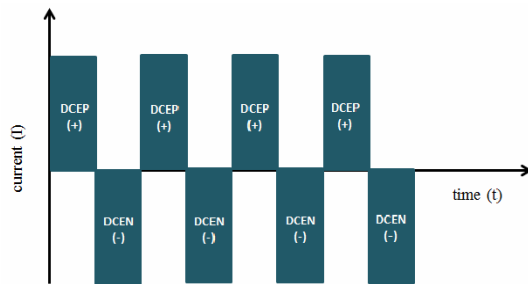


Fig. 1. Wave pattern during variable polarity welding.

Additional process variable of interesting besides the arc current, voltage and welding speed is DCEP duty ratio which is the portion of DCEP duration to one pulse period. The switching frequency, i.e. reverse of pulse period, is fixed to 100 Hz according to previous research which revealed switching frequency of several hundred Hz does not affect on welding quality. Welding process variables and contants related to arc are listed up in Table 2.

### 3. Results and discussion

With the aforementioned welding codition and analytic domain (4.6 cm \* 4 cm \* 0.8 cm, top 0.2 cm is void spcae for free surface expression, i.e. F value is zero), three dimensional numerical analysis of variable polarity arc weld pool is conducted. It contains temperature field analysis by conduction, phase transformation from solid to liquid, flow of molten pool and its free surface tracking. The simulation is acheived

Table 2. Arc welding parameters and related constants.

Property	Value
Current	150 A
Voltage	16 V
Welding speed	0.15 m/min
Switching freq.	100 Hz
$C_A$	2
$r_A$	3 mm
$\eta_{EN}$	0.7
$\eta_{rel}$ (3 levels)	1.000
	1.143
	1.286
$f_{(EP)}$ DCEP duty ratio (3 levels)	15%
	30%
	45%

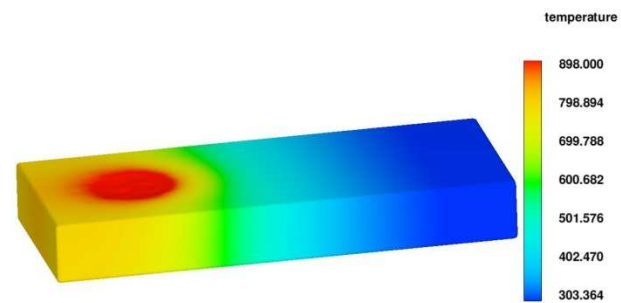


Fig. 2. Result of three dimensional molten pool analysis.

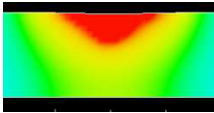
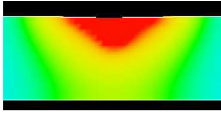
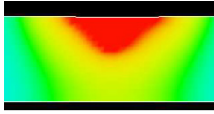
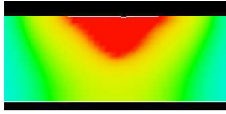
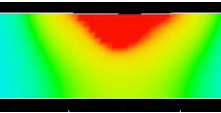
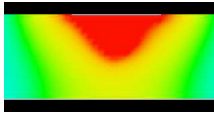
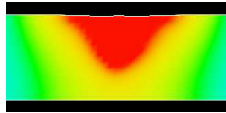
through commercial package Flow-3D. It provides basic solver for free surface tracking, continuity momentum and energy equations. The other features of arc welding and boundary conditions such as electromagnetic force, arc pressure, arc heat input and Maragnoi flow are implemented through user subroutines.

Representative screenshot of three dimensional simulation result is like Fig. 2. As seen in the figure, locally heated and melted zone exists and dimpled surface at the hottest area is observable which is due to arc pressure. Of course the simulation is transient therefore the hottest spot and supressed zone is moving along to the welding direction merely the figure is a still frame.

Fig. 3 is showing the transversial cross section imgae of weld pool. It is noticeable that there are flow vectors only in the molten area, i.e. FZ. It depicts also temperature distribution therefore it is also possible to predict HAZ (Heat affected zone) if a contour line of recrystallization temperature is drawn.

According to the previous experimental result, the cross sectional area of FZ was measured to estimate the amounts of the heat input in VP-GTAW of aluminum then it finally derived a graph depicts proportional relationship between FZ area and DCEP duty ratio. The same methodology is also

Table 3. Area of molten pool with variable polarity GTAW by the  $f_{(EP)}$ ,  $\eta_{rel}$ .

$f_{(EP)}$ \ $\eta_{rel}$	0.15	0.30	0.45	Remarks
1.0				DCEN
	10.40 mm <sup>2</sup>			
1.143				
	11.04 mm <sup>2</sup>	12.16 mm <sup>2</sup>	13.60 mm <sup>2</sup>	
1.286				
	12.16 mm <sup>2</sup>	14.56 mm <sup>2</sup>	17.76 mm <sup>2</sup>	

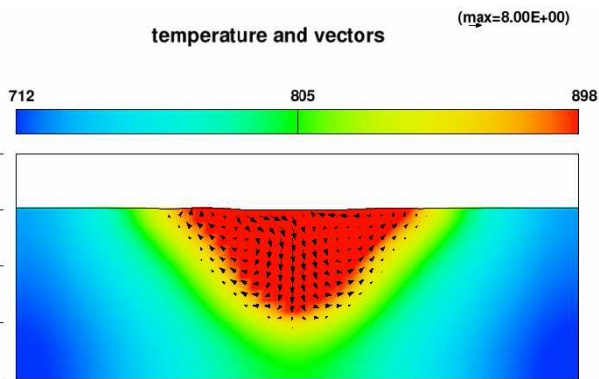


Fig. 3. Transvers cross section of molten pool analysis.

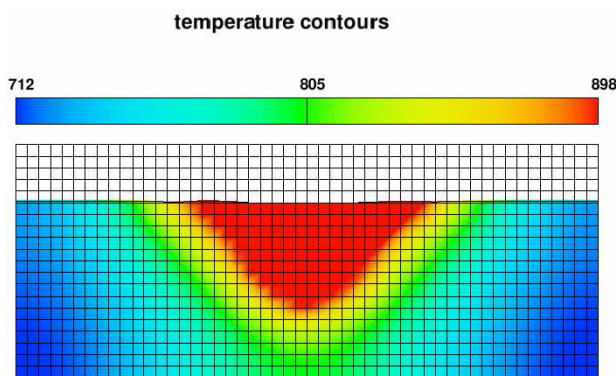


Fig. 4. The method to estimate the molten pool area.

adopted in this research to evaluate the heat input. As seen in Fig. 4, FZ area is roughly measured through counting the number of cells in the area. The simulation is in three dimensional space and analysis model is transient not steady state, therefore it should be careful to select a plane to measure FZ

area. In this simulation, the chosen plane is placed far enough from arc start point which guarantees that the weld pool is fully developed to become quasi steady state.

The final result of simulation is organized and listed up in Table 3. The cross sectional images are organized with respect to DCEP duty ratio,  $\eta_{rel}$  which is previously defined as relative heat input efficiency to DCEN. When the  $\eta_{rel}$  is equal to 1.0, the smallest weld pool area was shown because the DCEP heat input efficiency is same to DCEN so it is the lowest value we can presume. On the other hand, when the relative heat input efficiency and the DCEP duty ratio are 1.186 and 0.45 respectively, the maximum weld pool area was shown.

Accordingly it was confirmed that the higher  $f_{(EP)}$  or  $\eta_{rel}$ , the higher the heat input.

Result of above paragraph and Table 3 is clear because the simulation is designed in that way. This research is not dealing the problem in this simple way which shows only the feasibility of simulation. As introduced in chapter 1, the main purpose of the research is establishment of methodology to derive heat input efficiency of reverse polarity arc welding of aluminum. The simplest way is just tuning up  $\eta_{rel}$  to an single experimental result. However, this method contains complex ambiguity by two reasons. The first one is that the simulation model is built up on basis of several assumptions to simplify the equations and make it converge. No matter how accurately adjust the heat input efficiency, it contains inevitable errors due to the assumptions. The other reason is that the  $\eta_{EN}$  is not correct value but just an assumption which is used as basis for comparison. Therefore if we use higher  $\eta_{EN}$ , area of FZ will be larger so tuning up the absolute value of  $\eta_{rel}$  is essentially impossible.

The hint of suggested methodology is in Table 3 itself. As seen in the table, cross sections show larger FZ area for higher DCEP duty ratio. However the growth rate is not same but it depends on the  $\eta_{rel}$  value. Fig. 5 is a graph drawn by this man-

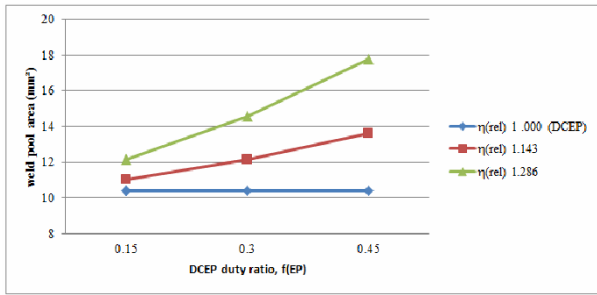


Fig. 5. The area of molten pool by the duty ratio of the DCEP.

ner. It shows the FZ area with respect to  $\eta_{rel}$  and DCEP duty ratio. As shown in the figure, the slope of each graph is different from each other regarding to  $\eta_{rel}$  value. The higher  $\eta_{rel}$ , the steeper slope. The previous experimental research presented the result in this manner. Therefore if we match the slope of the simulation to experiment, the  $\eta_{rel}$  value can be tuned up and this is the suggested methodology to determine the DCEP heat input efficiency through numerical analysis. Simulation of the present research is BOP (Bead on plate) model but the previous experiment was for lap joint fillet welding therefore further works will be aluminum BOP welding of VP-GTA and adjusting simulation to the experiment then finally determining DCEP arc heat input efficiency of aluminum.

#### 4. Conclusion

Several recent experimental studies about variable polarity arc welding of aluminum revealed that DCEP polarity has higher heat input than DCEN. However the phenomenon is contradict to conventional arc theory of anode heating. Although the theoretical background of the mechanism is still controversial, the phenomenon is clearly accepted by society. Hereby, numerical analysis model of variable polarity arc welding is developed and a methodology to determine the heat input efficiency by simulation is suggested through this research. The result successfully showed the feasibility of the simulation and the methodology and it can be summarized like following.

- (1) Simulation model of aluminum welding with newly suggested variable polarity arc heat source was developed and it successfully described the VP-GTAW of aluminum.
- (2) Relative heat input efficiency of DCEP polarity is introduced.
- (3) Cross sectional area of FZ in simulation is computed with respect to various relative heat input efficiency and duty ratio of DCEP polarity.
- (4) Methodology of DCEP heat input efficiency determination is suggested which can be accomplished through comparison of FZ area growth rate in simulation to experiment.
- (5) Furtherworks will be comparison of BOP aluminum welding with VP-GTA and simulation to determine the DCEP heat input efficiency.

#### Acknowledgement

This research was supported by Basic Science Research Program through the National Research Foundation of Korea (NRF) funded by the Ministry of Science, ICT and Future Planning, Korea (Grant No. 2012R1A1A1012487) and Technology Innovation Industrial Program funded by the Ministry of Trade, Industry & Energy, Korea (Grant No. 10052793).

#### Nomenclature

$B$	: Magnetic flux density
$B_r$	: Magnetic flux density in the r direction
$B_\theta$	: Magnetic flux density in the $\theta$ direction
$B_z$	: Magnetic flux density in the z direction
$C_A$	: Concentration coefficient of arc
$F$	: Volume fraction occupied by fluid
$F_r$	: Force in the r direction
$F_x$	: Force in the x direction
$F_y$	: Force in the y direction
$F_z$	: Force in the z direction
$F_\theta$	: Force in the $\theta$ direction
$g_z$	: Gravitational acceleration in the z direction
$h$	: Enthalpy
$h_A$	: Convection coefficient
$I$	: Welding current
$J$	: Current density
$J_r$	: Current density in the r direction
$J_\theta$	: Current density in the $\theta$ direction
$J_z$	: Current density in the z direction
$K$	: Thermal conductivity
$L_f$	: Latent heat of fusion
$n$	: Normal component
$P$	: Pressure
$P_A$	: Arc pressure
$q_{DC}$	: Energy given by direct current welding
$q_{DCEP}$	: Energy given during the DCEP
$q_{DCEN}$	: Energy given during the DCEN
$r_A$	: Effective radius of arc
$T$	: Temperature, a period
$T_l$	: Liquidus temperature
$T_s$	: Solidus temperature
$T_\infty$	: Ambient temperature
$t$	: Time
$t_{EP}$	: Time of DCEP during a cycle
$t_{EN}$	: Time of DCEN during a cycle
$u$	: Velocity component in the x direction
	: Internal energy
$V$	: Welding voltage, velocity
$\vec{V}$	: Velocity vector
$v$	: Velocity component in the y direction
$w$	: Velocity component in the w direction
$x, y, z$	: Cartesian coordinate index
$r, \theta, z$	: Cylindrical coordinate index

### Greek symbols

$\beta$	: Volume thermal expansion coefficient
$\gamma_s$	: Surface tension
$\varepsilon_s$	: Emissivity
$\eta_a$	: Heat input efficiency
$\eta_{EP}$	: Heat input efficiency during DCEP
$\eta_{EN}$	: Heat input efficiency during DCEN
$\eta_{rel}$	: Relative heat input efficiency ratio DCEP/DCEN
$\mu$	: Viscosity
$\mu_m$	: Magnetic permeability of metal
$\mu_0$	: Magnetic permeability in vacuum
$\pi$	: Circular constant
$\rho$	: Density
$\sigma$	: Normal stress
$\sigma_s$	: Stefan - Boltzmann constant
$\tau$	: Shear stress, surface tangent direction

### References

- [1] L. W. Eastwood, *Gases in Non-ferrous Metals and Alloys*, American Society for Metals, Cleveland, OH (1953).
- [2] J. Cho, Variable polarity plasma arc (VPPA) welding Part 1, Introduction and theoretical background, *Journal of Korean Welding and Joining Society*, 30 (2012) 199-201.
- [3] J. Cho, Variable polarity plasma arc (VPPA) welding Part 2, Applications and welding physics, *Journal of Korean Welding and Joining Society*, 30 (2012) 291-293.
- [4] H. Patte, R. Meister and R. Monroe, Cathodic cleaning and plasma arc welding of aluminum, *Welding Journal*, 47 (5) (1968) 226s-223s.
- [5] R. Sarrafi and R. Kovacevic, Cathodic cleaning of oxides from aluminum surface by variable-polarity arc, *Welding Journal*, 89 (2010) 1s-10s.
- [6] F. Li, Z. Yu, X. Xiao, X. Hua and Y. Wu, Research of Cathode Cleaning and Weld Formation of AC TIG Welding of Aluminum Alloy, *The 2nd East Asia Symposium on Technology*, Nara, Japan, Sep. 26-27 (2012).
- [7] M. A. R. Yarmuch and B. M. Patchett, Variable AC polarity GTAW fusion behavior in 5083 aluminum, *Welding Journal*, 86 (2007) 196s-200s.
- [8] J. Cho, Weldability increase of aluminum by variable polarity arc, *Journal of Korean Welding and Joining Society*, 32-1 (2014) 108-111.
- [9] J. Cho, J. Lee and S. Bae, Heat input analysis of variable polarity arc welding of aluminum, *International Journal of Advanced Manufacturing Technology*, 81 (2015) 1273-1280.
- [10] J. Cho, J. Lee, S. Bae, Y. Lee, K. Park, Y. Kim and J. Lee, Theoretical background discussion on variable polarity arc welding of aluminum, *Journal of Korean Welding and Joining Society*, 2 (2015) 14-17.
- [11] J. Cho, An analysis of three-dimensional molten pool in laser-GMA hybride welding, *Ph.D. Thesis*, KAIST, Korea (2007).
- [12] J. Cho, D. F. Farson, J. O. Milewski and K. J. Hollis, Weld pool flows during initial stages of keyhole formation in laser welding, *Journal of Physics D: Applied Physics*, 42 (2009) 175502.
- [13] J. Cho and S. J. Na, Implementation of real-time multiple reflection and Fresnel absorption of laser beam in keyhole, *Journal of Physics D: Applied Physics*, 39 (2006) 5372-5378.
- [14] J. Cho and S. J. Na, Theoretical analysis of keyhole dynamics in polarized laser drilling, *Journal of Physics D: Applied Physics*, 40 (2007) 7638-7647.
- [15] J. Cho and S. J. Na, Three-Dimensional Analysis of Molten Pool in GMA-Laser Hybrid Welding, *Welding Journal*, 88 (2009) 35s-43s.
- [16] J. Cho, D. F. Farson, K. J. Hollis and J. O. Milewski, Numerical analysis of weld pool oscillation in laser welding, *Journal of Mechanical Science and Technology*, 29 (4) (2015) 1715-1722.
- [17] Y. C. Lim, X. Yu, J. Cho, J. Sosa, D. F. Farson, S. S. Babu, S. McCracken and B. Flesner, Effect of magnetic stirring on grain structure refinement Part 1 - Autogenous nickel alloy welds, *Science and Technology of Welding and Joining*, 15 (2010) 583-589.
- [18] Y. C. Lim, X. Yu, J. Cho, J. Sosa, D. F. Farson, S. S. Babu, S. McCracken and B. Flesner, Effect of magnetic stirring on grain structure refinement Part 2 - Nickel alloy weld overlays, *Science and Technology of Welding and Joining*, 15 (2010) 400-406.
- [19] C. W. Hirt and B. D. Nichols, Volume of fluid method for the dynamics of free boundaries, *Journal of Computational Physics*, 39 (1981) 201s-225s.
- [20] R. W. Fox and A. T. McDonald, *Introduction to Fluid Mechanics*, 4th Ed., New York: Wiley (1992).
- [21] Z. Cao, Z. Yang and X. L. Chen, Three-dimensional simulation of transient GMA weld pool with free surface, *Welding Journal*, 83 (2004) 169s-176s.
- [22] A. Kumar and T. Debroy, Calculation of three-dimensional electromagnetic force field during arc welding, *Journal of Applied Physics*, 94 (2003) 1267-1277.



**Jungho Cho** received his Ph.D. at KAIST in 2007 and now he is a faculty of Chungbuk National University after working at Hyundai Motors for several years. His major is development of welding and joining techniques, welding physics and thermo-dynamical analysis of weld pool.